HHS Public Access

Author manuscript

Eur J Pharmacol. Author manuscript; available in PMC 2019 September 05.

Published in final edited form as:

Eur J Pharmacol. 2018 September 05; 834: 77–83. doi:10.1016/j.ejphar.2018.07.014.

Expression of active matrix metalloproteinase-9 as a likely contributor to the clinical failure of aclerastide in treatment of diabetic foot ulcers

Trung T. Nguyen[a], **Derong Ding**[a], **William R. Wolter**[b], **Matthew M. Champion**[a], **Dusan Hesek**[a], **Mijoon Lee**[a], **Rocio L. Pérez**[a], **Valerie A. Schroeder**[b], **Mark A. Suckow**[b,c], **Shahriar Mobashery**[a], and **Mayland Chang**[a,*]

[a]Department of Chemistry and Biochemistry, University of Notre Dame, Notre Dame, IN, USA

[b]Freimann Life Sciences Center and Department of Biological Sciences, University of Notre Dame, Notre Dame, IN, USA

[c]Present address: Veterinary Population Medicine Department, College of Veterinary Medicine, University of Minnesota, St. Paul, MN, USA

Abstract

Chronic wounds are a complication of diabetes. Treatment for diabetic foot ulcers is complex with little clinical recourse, resulting in 108,000 lower-limb amputations annually in the United States alone. Matrix metalloproteinases (MMPs) play important roles in the pathology and in the repair of chronic wounds. We previously identified active MMP-8 and MMP-9 in wounds of diabetic mice and determined that MMP-8 accelerates wound repair, while MMP-9 is the culprit for the diabetic wound being refractory to healing. Aclerastide, a peptide analog of angiotensin II, recently failed in phase III clinical trials for treatment of diabetic foot ulcers. We demonstrate herein that treatment of wounds of diabetic mice with aclerastide results in elevated levels of reactive oxygen species and of active MMP-9, which is likely an important contributor to the failure of aclerastide in clinical trials.

Graphical Abstract:

*To whom correspondence should be addressed. : mchang@nd.edu.

Declarations of Interest

The authors declare that US patent 9,604,957 has been issued for ND-336.

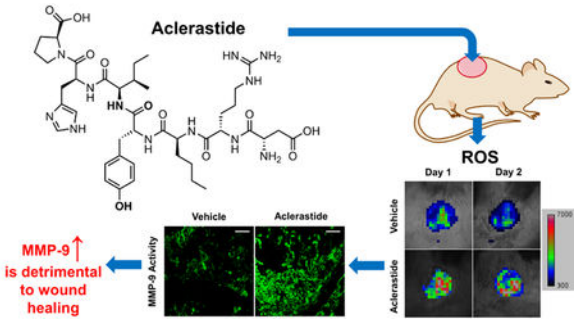

Keywords

matrix metalloproteinase-9; aclerastide; diabetic foot ulcers; reactive oxygen species, angiotensin II

1. Introduction

Diabetes affects over 30 million individuals in the United States (Centers for Disease Control and Prevention, 2017). A challenging problem in diabetes is the inability of wounds to heal, with 25% of diabetic patients developing diabetic foot ulcers (DFUs) over their lifetimes (Rice et al., 2014). The standard-of-care for DFUs is debridement, off-loading, and treatment of wound infections with antibiotics. There is a single FDA-approved drug, becaplermin (Regranex™); however, it is not the standard-of-care in DFU treatment due to its modest efficacy and black-box warning (Margolis et al., 2005; Ziyadeh et al., 2011). The dearth of treatment options for DFUs results in 108,000 lower-limb amputations annually in the United States (Centers for Disease Control and Prevention, 2017) and prognosis with approximately 50% mortality within one year of amputation (Fortington et al., 2013).

Matrix metalloproteinases (MMPs) play important roles in both the pathology and repair of chronic wounds (Chang, 2016; Nguyen et al., 2016). The molecular basis of why the diabetic wound is recalcitrant to healing and which MMP(s) accelerates wound healing is not fully understood (Nguyen et al., 2016). There are 24 human MMPs and each MMP exits in three forms (Nguyen et al., 2016), of which only the active unregulated MMPs play catalytic roles in physiological and pathophysiological processes. The majority of the methods for profiling MMPs cannot distinguish among the three forms of MMPs (Fisher and Mobashery, 2010). In addition, these methods often require screening for a specific MMP rather than “fishing” out and identifying the active MMP(s) that plays critical roles in repair and disease.

To address this challenge, we developed an affinity resin (Hesek et al., 2006) that binds only to active MMPs, which are then identified by mass spectrometry (Gooyit et al., 2014). Using this affinity resin we identified active MMP-8 and MMP-9 in wounds of *db/db* mice (Gooyit et al., 2014). We documented that MMP-9 was detrimental to wound healing and that MMP-8 played a beneficial role in repairing the wound (Gao et al., 2015; Gooyit et al., 2014). We also identified a small-molecule selective MMP-9 inhibitor referred to as ND-336 that accelerated diabetic wound healing (Gao et al., 2015). These findings for the first time

identified MMP-9 as a target in DFUs, one that addressed the molecular basis of disease, rather than merely serving a palliative purpose.

We were keenly interested in a new drug for diabetic wound healing, aclerastide (NorLeu^{3}-angiotensin(1–7) or DSC127), which entered phase III clinical trials in 2013. Aclerastide is a peptide analog of angiotensin II, a growth factor (Vukelic and Griendling, 2014) that plays an important role in wound healing (Yahata et al., 2006). Aclerastide had shown superior efficacy over becaplermin in the *db/db* mouse model of wound healing (n = 5 mice per group), when given topically at 0.1 mg/wound/day for 5 days starting immediately after injury (Rodgers et al., 2003), but in November of 2015 it failed in phase III clinical trials for the treatment of DFUs, where it was applied once daily for several weeks.

Angiotensin II mediates cell growth by stimulating NADPH oxidase (Griendling and Ushio-Fukai, 2000), producing reactive oxygen species after tissue injury (Mehta and Griendling, 2007). Reactive oxygen species is known to promote activation of MMP-9 (Gu et al., 2002) via NF-κB regulation. We theorize that aclerastide might stimulate formation of reactive oxygen species, which would in turn upregulates MMP-9. In light of the detrimental role that we have documented for MMP-9 in diabetic wounds, we wondered if a contributor to the clinical failure could be the effect of aclerastide on MMP-9 upregulation.

2. Materials and Methods

2.1. Compounds

Aclerastide (NorLeu^{3}-angiotensin(1–7)) was custom-synthesized by GenScript; purity 98.6% by HPLC. Peptide sequence Asp-Arg-NorLeu-Tyr-Ile-His-Pro was confirmed by MS/MS analysis on a Bruker micrOTOF/Q2 mass spectrometer. High-resolution mass spectra were measured using a Bruker micrOTOF/Q2 mass spectrometer in electrospray ionization (ESI). HRMS $[M + H]^{+}$ calcd for $C_{42}H_{65}N_{12}O_{11}$ 913.4890; found 913.4894. ND-336 was synthesized as previously described (Gao et al., 2015).

2.2. Animal model

Female *db/db* mice (BKS.Cg-*Dock7*$^{m\ +/+}$ *Lepr*^{db}/J, 8-weeks old, about 40 grams body weight) were purchased from Jackson Laboratory. Animals were fed 501 Laboratory Rodent Diet and were given water *ad libitum*. The mice were housed in polycarbonate cages (one animal per cage) containing corncob bedding (The Andersons Inc.) and maintained at 72 ± 2 °F with a light/dark cycle of 12/12 h. All animal studies were conducted in accordance with the National Institutes of Health guide for the care and use of laboratory animals, and with approval and oversight by the Institutional Animal Care and Use Committee at the University of Notre Dame. All animal studies complied with the ARRIVE guidelines.

Mice were shaved in the dorsal area, prepared for aseptic surgery, and anesthetized with isoflurane in early morning. A single 8-mm diameter full-thickness excisional wound was created on the dorsal area using a biopsy punch (Miltex) and it was covered with Tegarderm dressing (3M Company). The next day (day 1), the animals were randomly assigned to different experimental groups. A sample size of n = 7 animals per group was estimated to have 80% power to give 20% improvement in wound closure, with a statistical significance

of 0.05. Body weight was monitored before and during the experiments; no significant weight loss (≥ 20% body weight) was observed. Mice were excluded from the studies if body weight was < 32 g or blood glucose was < 250 mg/dl, indicating that the animals were not diabetic. At specific time points or at the end of the study, mice were euthanized by isoflurane inhalation overdose, followed by cervical dislocation.

2.3. Aclerastide and ND-336 study

This study consisted of three groups of *db/db* mice (37.5 ± 3 g body weight): n = 13 mice for vehicle, n = 12 mice for aclerastide, n = 12 mice for ND-336 as positive control. Aclerastide and ND-336 were dissolved in water at a concentration of 1.0 mg/ml; the vehicle consisted of distilled sterile water. The aclerastide, ND-336, and vehicle solutions were sterile-filtered and stored at 4 °C. Dosing solutions were prepared freshly every 2 days and warmed to room temperature before dosing. Mouse wounds were topically administered 100 μl of aclerastide, ND-336, or vehicle solutions once a day in the morning for 14 days. The dose of aclerastide and ND-336 was equivalent to 0.1 mg/wound/day. Treatments were started one day post-injury (day 1) in the order: vehicle, aclerastide, and ND-336. Wounds were measured on days 0, 7, 10, and 14. Mice (n = 3 per group) were killed on day 7, the wounds were harvested and frozen in liquid nitrogen and stored at −80 °C for gelatin zymography and affinity resin analysis.

2.4. Wound measurements

The mice were briefly anesthetized with isofluorane via inhalation and the wounds were photographed using a Nikon D5300 camera mounted on a tripod at a fixed distance; a ruler was included in the photographic frame. Wound areas were calculated using NIH ImageJ software (version 1.51). The wound closure analysis was performed separately by two experimenters, one of whom was blinded. Wound healing is reported as percent change in wound area relative to day 0. Wounds were measured and analyzed consecutively by animal number.

2.5. In vivo imaging for reactive oxygen species

A separate study was conducted with 15 *db/db* mice: n = 6 for vehicle and aclerastide, and n = 3 for ND-336. Excisional wounds were treated topically with vehicle, aclerastide, or ND-336 as described earlier once a day for 2 days. Mice were anesthetized with 2% isoflurane via inhalation on days 1 and 2 after wound infliction. The mice (n = 3 per group per time point) were intraperitoneally injected with 200 μl of L-012 (Soares et al., 2016) (Wako Chemicals) dissolved in PBS at 5 mg/ml. The images were acquired immediately, and at 5-min intervals using a Xenogen IVIS Lumina instrument (Caliper Life Sciences), controlled with *Living Image* software (v 3.0). The bioluminescent images were analyzed and quantified by *ImageJ* software version 1.51. Mice (n = 3 per group) were euthanized on days 1 and 2 for affinity resin analysis.

2.6. In-situ zymography

A separate study consisting on 9 *db/db* mice (n = 3 mice per group) was carried out, in which excisional wounds were treated with vehicle, aclerastide, or ND-336 once a day for 2

days. Mice were euthanized on day 2, and wound tissues were harvested, embedded in optimum cutting temperature compound, and cryosectioned at 8-μm thickness for *in-situ* zymography, as described previously (Oh et al., 1999). Briefly, wound tissue sections were incubated for 1 h at room temperature with DQ-gelatin or DQ-collagen (ThermoFisher, diluted in 50 mM Tris-buffered saline, pH 7.6). After fixation in 4% paraformaldehyde in PBS, tissues were counterstained with 4,6-diamidino-2-phenylindole (DAPI) for visualization of nuclei and images were obtained using confocal microscopy. Blinded analysis was performed using *ImageJ* software.

2.7. Affinity resin

The affinity resin was synthesized in 14 synthetic steps using a previously reported method (Hesek et al., 2006).

2.8. Analysis of diabetic wounds by affinity resin coupled with proteomics

Wound samples (100 mg) on days 1, 2, and 7 were homogenized in 1000 μl of cold lysis buffer (25 mM Tris·HCl pH 7.5, 100 mM NaCl, 1% v/v Nonidet P-40) using a Bullet Blender (Next Advance); protein concentration in the homogenates was determined by the BCA assay (Walker, 2009). A 10-mg aliquot of tissue homogenate was incubated with 100 μl of the affinity resin at 4 °C for 2 h. After centrifugation (12000*g*, 20 min, 2x), internal standard (150 fmol/mg tissue of yeast enolase) was added to the resin beads in the pellet, followed by reduction of disulfide bonds in MMPs (100 mM dithiothreitol, 65 °C, 30 min), and alkylation to prevent disulfide bonds from reforming (100 mM iodoacetamide, room temperature, 20 min). The resin-bound MMPs were trypsin digested (0.2 μg in 50 mM ammonium bicarbonate) at 37 °C overnight and desalted through Millipore ZipTip®. An aliquot of the desalted peptide mixture was analyzed on a nanoUPLC instrument (Waters Corporation) coupled to a Thermo LTQ Velos Orbitrap tandem mass spectrometer (Thermo Fisher Scientific) and analyzed by ESI. A Waters nanoACQUITY 1.7 μm, BEH120 C18, 100 μm i.d. x 10 cm column was used, flow rate of 800 nl/min, 5 min 1% A/99% B, 45-min linear gradient to 60% A/40% B, 5-min linear-gradient to 85% A/15% B, where A = 0.1% formic acid in acetonitrile and B = 97% water/3% acetonitrile/0.1% formic acid. Identification of active MMPs was done using MS/MS spectral information and the Uniprot database. Quantitative methods were developed using the label-free multiple-reaction monitoring (MRM) method using a 6500 QTrap mass spectrometer (AB Sciex LLC) interfaced with Protein Pilot software (v. 5.0, AB Sciex LLC) using three peptides (custom-synthesized by GenScript) per MMP. The synthesized peptides used for identifying and quantifying MMPs in mouse wounds are shown in Table 1. Levels of active MMPs in the wound samples were determined from the calibration curves containing known amounts of synthetic peptides in blank mouse tissue relative to internal standard, using three peptides per MMP, with three transitions as qualifiers to identify the protein and three transitions as quantifiers to quantify the MMPs.

2.9. Gelatin zymography

Aliquots of the tissue extracts containing 0.5 mg of protein were affinity precipitated with gelatin-Agarose beads, followed by treatment with 2% sodium dodecyl sulfate to release the bound gelatinases from the beads. The samples were analyzed by electrophoresis in a 10%

gelatin zymogram gel, as previously described (Toth and Fridman, 2001). Gelatin zymography was performed on n = 3 mice per group on day 7.

2.10. Statistical analysis

Data for n ≥ 7 are expressed as mean ± S.E.M. and for n < 7 as mean ± S.D. Data were analyzed for statistical significance using the Mann Whitney *U* test for n ≥ 7 with two-tailed hypothesis, or the Student's *t* test for n < 7 with two-tailed hypothesis.

3. Results

3.1. Aclerastide does not accelerate wound healing in db/db mice

We evaluated aclerastide (Fig. 1A) in an excisional mouse model of wound healing using *db/db* mice, with the selective MMP-9 inhibitor ND-336 (Gao et al., 2015) (Fig. 1A) as positive control. The wounds were topically treated once daily with aclerastide or ND-336 starting one day after wound infliction; a vehicle control (water) was included. Wound healing is summarized in Fig. 1B and representative images of the wounds are shown in Fig. 1C. Wound healing in aclerastide-treated mice was similar to that in vehicle-treated controls, with no statistically significant differences ($P > 0.05$) observed during the 14-day course of the study. In contrast, mice treated with ND-336 showed significant acceleration of wound healing on days 10 and 14 relative to vehicle ($P = 0.008$ and 0.0001 on days 10 and 14, respectively) and aclerastide ($P = 0.007$ and 0.008 on days 10 and 14, respectively). Wounds treated with ND-336 healed faster on day 7 compared to vehicle, although the differences were not statistically significant ($P = 0.052$).

3.2. Aclerastide upregulates reactive oxygen species during inflammation

Since angiotensin II has been reported to upregulate reactive oxygen species, we imaged the wounds with L-012, a chemiluminescent luminol analog for detection of NADPH oxidase-derived superoxide (Zielonka et al., 2013). ND-336 was included as a positive control. Increased levels of reactive oxygen species were observed in aclerastide-treated wounds on days 1 and 2 after wound infliction, compared to vehicle (Fig. 2A). Aclerastide treatment upregulated reactive oxygen species by 3-fold on day 1 and 2.4-fold on day 2, respectively (Fig. 2B). On the contrary, ND-336 lowered reactive oxygen species levels in the diabetic wounds by 1.9-fold on day 2 (Fig. 2A and 2B). The decrease of reactive oxygen species upon treatment with ND-336 is consistent with its demonstrated reduction of inflammation (Gao et al., 2015).

3.3. Aclerastide increases the levels of the detrimental active MMP-9 in diabetic wounds

Since reactive oxygen species is known to induce the expression of MMP-9 in vascular smooth muscle cells (Guo et al., 2008), we investigated the activity of MMP-9 in wounds collected on day 7 by gelatin zymography. No differences were observed in active MMP-9 bands in aclerastide-treated wounds compared to vehicle. A drawback of gelatin zymography is that the sodium dodecyl sulfate used in this technique dissociates TIMP-complexed MMPs resulting in a false positive active band. Therefore, we conducted an additional study in which wounds were analyzed by *in-situ* zymography, a technique that detects only active proteinase activity in tissue sections using fluorescent substrates

(Vandooren et al., 2013), where proteolytic activity is observed as fluorescence. We used dye-quenched (DQ)-gelatin, a substrate for gelatinases (MMP-2 and MMP-9) and DQ-collagen, a substrate for collagenases (MMP-8 and MMP-13). MMP-8 has been shown to play a beneficial role in diabetic wound healing (Gao et al., 2015; Gooyit et al., 2014). Since MMP-2 and MMP-13 are not detected in *db/db* mouse wounds (Gooyit et al., 2014), only MMP-9 and MMP-8 activities are visualized in the wound milieu. Wounds in *db/db* mice treated with aclerastide show upregulation of MMP-9 activity on day 2, whereas ND-336 inhibits the activity of this detrimental proteinase (Fig. 3A). Both aclerastide-treated and ND-336-treated wounds show no discernable effect on MMP-8 activity (Fig. 3B). Since proteinase activity by *in-situ* zymography is not quantitative (Vandooren et al., 2013), we analyzed the aclerastide-treated wounds using our affinity resin coupled with proteomics.

In order to confirm the upregulated levels of MMP-9, we analyzed the wounds by our affinity resin coupled with proteomics. This technique detects and quantifies only active MMPs, and not the zymogens or TIMP-complexed MMPs. The only active MMPs observed with the affinity resin were MMP-8 and MMP-9. Levels of active MMP-9 were 8.1 ± 2.1 and 9.5 ± 1.8 fmol/mg tissue for vehicle and 22.3 ± 4.9 and 23.8 ± 5.5 fmol/mg tissue for aclerastide on days 1 and 2, respectively (Fig. 4A), 2.7- and 2.5-fold increases, which were statistically significant ($P = 0.024$ and $P = 0.037$, respectively). Although 2.5-fold higher levels of active MMP-8 were observed in wounds treated with aclerastide (Fig. 4B) on day 1, compared to vehicle-treated wounds, these differences were not statistically significant ($P = 0.08$). We did not analyze ND-336-treated wounds since ND-336 is not a covalent inhibitor of MMP-9, and it will dissociate from the active site during incubation with the affinity resin.

4. Discussion

Diabetes is the world's most prevalent metabolic disease, affecting 382 million patients globally in 2013 and that number will reach 592 million individuals by 2035 (Guariguata et al., 2014). One out of four diabetic patients is affected by DFUs, a common complication of diabetes (Rice et al., 2014). With the projected increase in the number of diabetics, DFUs will also be on the rise beyond the current number of 900,000 ulcers and 108,000 lower-limb amputations that occur annually in the United States (Centers for Disease Control and Prevention, 2017). Furthermore, the reoccurrence of DFUs in diabetic patients is common, with the rate of 40% recurring within one year and 60% within three years (Armstrong et al., 2017). The standard-of-care for treatment of DFUs is not sufficient to stimulate healing of DFUs and contributes to the rise in amputations. Becaplermin remains the only FDA-approved drug since it was launched 20 years ago; however, this drug has modest efficacy, and it is seldom prescribed because of its side effects (Ziyadeh et al., 2011). A different approach is the use of skin substitutes such as Apligraf® and Dermagraft®, however they are contraindicated for infected DFUs, and were found to have modest improvement over the standard-of-care (Greer et al., 2013). Unfortunately, the survival rate of diabetic amputees is only 50% after one year of amputation (Fortington et al., 2013). There is a critical need to develop new therapeutic treatments for DFUs.

A common strategy to stimulate tissue healing in DFUs is the use of growth factors. There have been at least 28 randomized clinical trials to assess the efficacy of 11 different growth factors over the years, including platelet-derived growth factor (becaplermin), recombinant human epidermal growth factor, and recombinant human VEGF (Marti-Carvajal et al., 2015). While there is no clear evidence that treatment with growth factors can reduce the number of lower-limb amputations in DFUs, growth factors show increased risks of adverse effects (Marti-Carvajal et al., 2015). Becaplermin promotes angiogenesis, and has a black-box warning for increased risk of cancer and death. Aclerastide is an analog peptide of the growth factor angiotensin II, which promotes angiogenesis (Tamarat et al., 2002) and induces migration of fibroblasts and keratinocytes that promote wound healing (Yahata et al., 2006). However, angiotensin II also produces reactive oxygen species (Mehta and Griendling, 2007), that is known to upregulate MMP-9 (Gu et al., 2002). As MMP-9 plays a detrimental role in diabetic wound healing (Gao et al., 2015; Gooyit et al., 2014), we investigated whether aclerastide might promote production of reactive oxygen species and upregulation of MMP-9, which may have contributed to the failure of aclerastide in clinical trials for the treatment of DFUs.

We used the *db/db* mouse model, which is widely used to study wound healing, as delayed wound healing has been demonstrated in this model (Sullivan et al., 2004). Furthermore, *db/db* mice have an autosomal recessive mutation that causes leptin receptors in the hypothalamus to be defective (Sullivan et al., 2004). This results in obesity and hyperglycemia that mimics type 2 diabetes in humans. Wounds in *db/db* mice heal by re-epithelialization (Sullivan et al., 2004), resembling healing of human wounds, where keratinocytes migrate at the margins of the wounds. A limitation of this animal model is that it is a delayed wound-healing model, whereas human DFUs are chronic. However, all existing animal models are delayed wound-healing models.

The efficacy of ND-336 in the current study was similar to that reported earlier (Gao et al., 2015). While the previous study by Rodgers *et al.* and the current study used the same topical route of administration, the same dose level (100 ng/wound/day) and dose frequency (once a day), the previous study initiated aclerastide treatment immediately after injury for 5 days (Rodgers et al., 2003), whereas the present study started treatment 24 h after injury for 14 days. We also used twice as many mice as were employed in the Rodgers' study. Aclerastide had shown efficacy in *db/db* mice when administered topically immediately after wound infliction and when given for a short period of 5 days (Rodgers et al., 2003). However, we demonstrated that aclerastide does not accelerate wound healing when applied topically to wounds of *db/db* mice starting one day after injury once a day for 14 days, a dosing regimen that more closely resembles the clinical usage. Interestingly, aclerastide-treated wounds healed comparable to vehicle and not worse than vehicle. This can be explained by a balance between the beneficial effect of aclerastide in promoting angiogenesis and inducing fibroblast and keratinocyte migration that promote wound healing (Tamarat et al., 2002; Yahata et al., 2006) and the detrimental effect of aclerastide in upregulating MMP-9 that delays wound healing. The net effect is that one counteracts the other, resulting in aclerastide-treated wounds that heal similar to vehicle.

In normal wound healing, inflammatory cells generate reactive oxygen species immediately after wound injury to defend against pathogen invasion, and to stimulate the production of proteinases such as MMPs that remodel the extracellular matrix (Nguyen et al., 2016). However, uncontrolled upregulation of reactive oxygen species in the wound hypoxic environment can cause tissue destruction and hinder the repair processes (Gary Sibbald and Woo, 2008). We further demonstrated that treatment with aclerastide resulted in increased levels of reactive oxygen species and higher levels of active MMP-9, the latter of which is detrimental to wound healing, and is likely a contributing factor to the failure of aclerastide in phase III clinical trials. Our findings are in agreement with studies of chronic wounds in diabetic patients, where the excessive production of reactive oxygen species has been found to subsequently increase MMP levels by 60-fold over those in healing wounds (Guo and Dipietro, 2010).

Acknowledgments

Funding

This work was supported by the American Diabetes Association Pathway to Stop Diabetes (grant 1–15-ACN-06). TTN is a Ruth L. Kirschtein National Research Service Award Fellow of the Chemistry-Biochemistry-Biology Interface Program at the University of Notre Dame, supported by training grant T32 GM075762 from the National Institutes of Health.

REFERENCES

Armstrong DG, Boulton AJM, Bus SA, 2017 Diabetic Foot Ulcers and Their Recurrence. N. Engl. J. Med 376, 2367–2375. [PubMed: 28614678]

Centers for Disease Control and Prevention., 2017 National Diabetes Statistics Report: Estimate of diabetes and its burden in the United States.

Chang M, 2016 Restructuring of the extracellular matrix in diabetic wounds and healing: A perspective. Pharmacol. Res 107, 243–248. [PubMed: 27033051]

Fisher JF, Mobashery S, 2010 Mechanism-based profiling of MMPs, in: Clark IM, Young DA, Rowan AD (Eds.), Matrix Metalloproteinase Protocols 2nd ed. Humana Press, New York, pp. 471–487.

Fortington LV, Geertzen JH, van Netten JJ, Postema K, Rommers GM, Dijkstra PU, 2013 Short and long term mortality rates after a lower limb amputation. Eur. J. Vasc. Endovasc. Surg 46, 124–131. [PubMed: 23628328]

Gao M, Nguyen TT, Suckow MA, Wolter WR, Gooyit M, Mobashery S, Chang M, 2015 Acceleration of diabetic wound healing using a novel protease-anti-protease combination therapy. Proc. Natl. Acad. Sci. U. S. A 112, 15226–15231. [PubMed: 26598687]

Gary Sibbald R, Woo KY, 2008 The biology of chronic foot ulcers in persons with diabetes. Diabetes Metab. Res. Rev 24 Suppl 1, S25–30. [PubMed: 18442179]

Gooyit M, Peng Z, Wolter WR, Pi H, Ding D, Hesek D, Lee M, Boggess B, Champion MM, Suckow MA, Mobashery S, Chang M, 2014 A chemical biological strategy to facilitate diabetic wound healing. ACS Chem. Biol 9, 505–510.

Greer N, Foman NA, MacDonald R, Dorrian J, Fitzgerald P, Rutks I, Wilt TJ, 2013 Advanced wound care therapies for nonhealing diabetic, venous, and arterial ulcers: a systematic review. Ann. Intern. Med 159, 532–542. [PubMed: 24126647]

Griendling KK, Ushio-Fukai M, 2000 Reactive oxygen species as mediators of angiotensin II signaling. Regul Pept 91, 21–27. [PubMed: 10967199]

Gu Z, Kaul M, Yan B, Kridel SJ, Cui J, Strongin A, Smith JW, Liddington RC, Lipton SA, 2002 S-nitrosylation of matrix metalloproteinases: signaling pathway to neuronal cell death. Science 297, 1186–1190. [PubMed: 12183632]

Guariguata L, Whiting DR, Hambleton I, Beagley J, Linnenkamp U, Shaw JE, 2014 Global estimates of diabetes prevalence for 2013 and projections for 2035. Diabetes Res. Clin. Pract 103, 137–149. [PubMed: 24630390]

Guo RW, Yang LX, Wang H, Liu B, Wang L, 2008 Angiotensin II induces matrix metalloproteinase-9 expression via a nuclear factor-kappaB-dependent pathway in vascular smooth muscle cells. Regul. Pept 147, 37–44. [PubMed: 18252266]

Guo S, Dipietro LA, 2010 Factors affecting wound healing. J. Dent. Res 89, 219–229. [PubMed: 20139336]

Hesek D, Toth M, Krchnak V, Fridman R, Mobashery S, 2006 Synthesis of an inhibitor-tethered resin for detection of active matrix metalloproteinases involved in disease. J. Org. Chem 71, 5848–5854. [PubMed: 16872162]

Margolis DJ, Bartus C, Hoffstad O, Malay S, Berlin JA, 2005 Effectiveness of recombinant human platelet-derived growth factor for the treatment of diabetic neuropathic foot ulcers. Wound Repair Regen. 13, 531–536. [PubMed: 16283867]

Marti-Carvajal AJ, Gluud C, Nicola S, Simancas-Racines D, Reveiz L, Oliva P, Cedeno-Taborda J, 2015 Growth factors for treating diabetic foot ulcers. Cochrane Database Syst Rev, CD008548. [PubMed: 26509249]

Mehta PK, Griendling KK, 2007 Angiotensin II cell signaling: physiological and pathological effects in the cardiovascular system. Am. J. Physiol. Cell Physiol. 292, C82–97. [PubMed: 16870827]

Nguyen TT, Mobashery S, Chang M, 2016 Roles of matrix metalloproteinases in cutaneous wound healing, in: Alexandrescu VA (Ed.), Wound Healing: New Insights into Ancient Challenges. InTech, pp. 37–71.

Oh LYS, Larsen PH, Krekoski CA, Edwards DR, Donovan F, Werb Z, Yong VW, 1999 Matrix metalloproteinase-9/gelatinase B is required for process outgrowth by oligodendrocytes. J. Neurosci 19, 8464–8475. [PubMed: 10493747]

Rice JB, Desai U, Cummings AK, Birnbaum HG, Skornicki M, Parsons NB, 2014 Burden of diabetic foot ulcers for medicare and private insurers. Diabetes Care 37, 651–658. [PubMed: 24186882]

Rodgers KE, Espinoza T, Felix J, Roda N, Maldonado S, diZerega G, 2003 Acceleration of healing, reduction of fibrotic scar, and normalization of tissue architecture by an angiotensin analogue, NorLeu3-A(1–7). Plast Reconstr Surg 111, 1195–1206. [PubMed: 12621191]

Soares MA, Cohen OD, Low YC, Sartor RA, Ellison T, Anil U, Anzai L, Chang JB, Saadeh PB, Rabbani PS, Ceradini DJ, 2016 Restoration of Nrf2 Signaling Normalizes the Regenerative Niche. Diabetes 65, 633–646. [PubMed: 26647385]

Sullivan SR, Underwood RA, Gibran NS, Sigle RO, Usui ML, Carter WG, Olerud JE, 2004 Validation of a model for the study of multiple wounds in the diabetic mouse (db/db). Plast. Reconstr. Surg 113, 953–960. [PubMed: 15108888]

Tamarat R, Silvestre JS, Durie M, Levy BI, 2002 Angiotensin II angiogenic effect in vivo involves vascular endothelial growth factor- and inflammation-related pathways. Lab. Invest 82, 747–756. [PubMed: 12065685]

Toth M, Fridman R, 2001 Assessment of Gelatinases (MMP-2 and MMP-9 by Gelatin Zymography. Methods Mol. Med 57, 163–174. [PubMed: 21340898]

Vandooren J, Geurts N, Martens E, Van den Steen PE, Opdenakker G, 2013 Zymography methods for visualizing hydrolytic enzymes. Nat Methods 10, 211–220. [PubMed: 23443633]

Vukelic S, Griendling KK, 2014 Angiotensin II, from vasoconstrictor to growth factor: a paradigm shift. Circ. Res 114, 754–757. [PubMed: 24577962]

Walker JM, 2009 The bicinchoninic acid (BCA) assay for protein quantification, in: Wlaker JM (Ed.), The Protein Protocols Handbook. Springer Protocols Handbook. Humana Press, Totowa, NJ.

Yahata Y, Shirakata Y, Tokumaru S, Yang L, Dai X, Tohyama M, Tsuda T, Sayama K, Iwai M, Horiuchi M, Hashimoto K, 2006 A novel function of angiotensin II in skin wound healing. Induction of fibroblast and keratinocyte migration by angiotensin II via heparin-binding epidermal growth factor (EGF)-like growth factor-mediated EGF receptor transactivation. J. Biol. Chem 281, 13209–13216. [PubMed: 16543233]

Zielonka J, Lambeth JD, Kalyanaraman B, 2013 On the use of L-012, a luminol-based chemiluminescent probe, for detecting superoxide and identifying inhibitors of NADPH oxidase: a reevaluation. Free Radic Biol Med 65, 1310–1314. [PubMed: 24080119]

Ziyadeh N, Fife D, Walker AM, Wilkinson GS, Seeger JD, 2011 A matched cohort study of the risk of cancer in users of becaplermin. Adv Skin Wound Care 24, 31–39. [PubMed: 21173589]

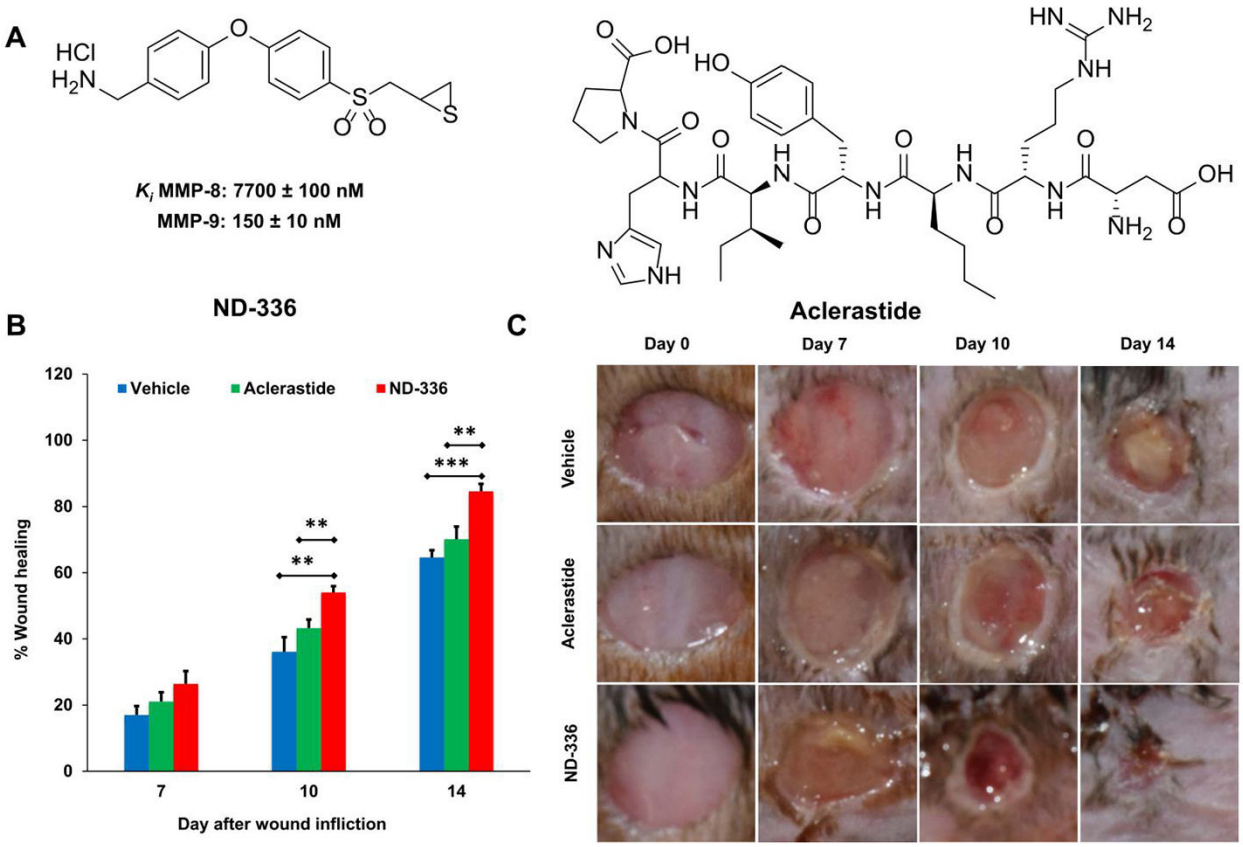

Fig. 1.

Aclerastide does not accelerate wound healing in *db/db* mice. A. Structures of ND-336 and aclerastide. Mice were given a single 8 mm diameter full-thickness excision wound on the dorsal thorax and the wounds were covered with Tegaderm dressing. Mice were treated topically one day later with ND-336 or aclerastide at 100 μg/wound/day for 14 days or vehicle (water). B. Wound closure measurements indicate that ND-336 accelerates wound healing faster than aclerastide; mean ± S.E.M., n = 12, 9, and 9 mice for ND-336 or aclerastide on days 7, 10, and 14, respectively; n = 13, 10, and 10 mice for vehicle on days 7, 10, and 14, respectively; $^{**}P < 0.01$, $^{***}P < 0.001$ by Mann-Whitney *U* two-tailed test. C. Representative images of the wounds.

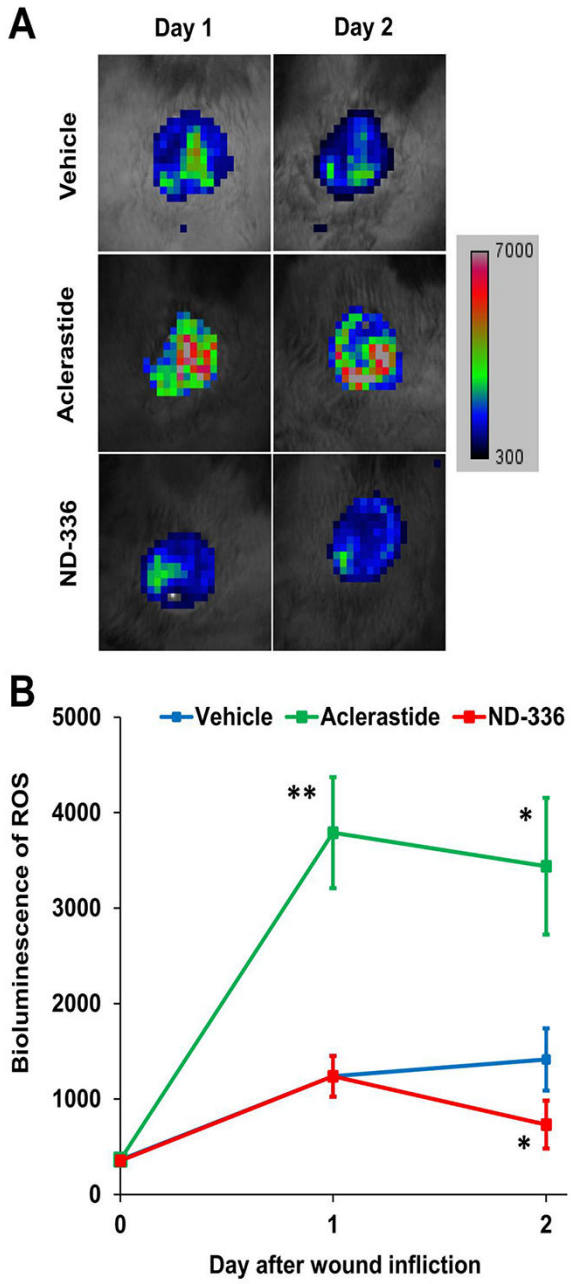

Fig. 2.

Aclerastide treatment results in increased levels of reactive oxygen species during the inflammation stage of wound healing. A. *In vivo* imaging for reactive oxygen species (25 mg/kg of L-012 intraperitoneally, n = 3 mice per group per time point) shows increased levels of reactive oxygen species in aclerastide-treated mice, whereas decreased levels of reactive oxygen species were observed in ND-336-treated mice. B. Bioluminescence quantification indicates a statistically significant upregulation of reactive oxygen species in aclerastide-treated mice on days 1 and 2, and a statistically significant reduction of reactive

oxygen species in ND-336 treated wounds on day 2; *$P < 0.05$, **$P < 0.01$ by Student's t two-tailed test.

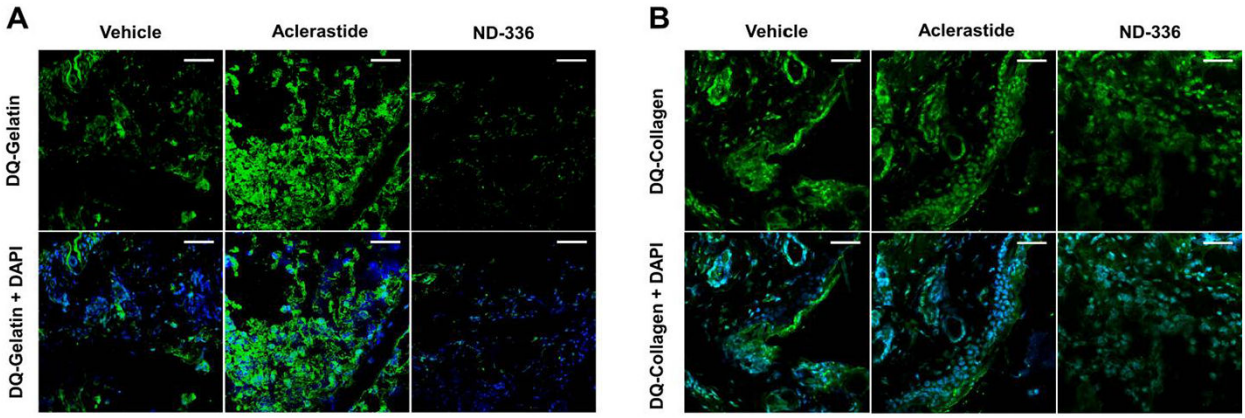

Fig. 3.

Aclerastide treatment increases the detrimental MMP-9 activity in diabetic wounds. Analysis of day 2 wound tissues by *in-situ* zymography (top panel, DQ-substate (activity denoted by fluorescent green); bottom panel DQ-substrate merged with nuclear DNA staining by DAPI (denoted in blue)), n = 3 mice per group. A. *In-situ* zymography with DQ-Gelatin indicates upregulated MMP-9 activity in aclerastide-treated wounds compared to vehicle, whereas MMP-9 activity was inhibited in ND-336-treated wounds. B. *In-situ* zymography with DQ-Collagen shows MMP-8 activity is not affected by treatment with aclerastide or ND-336. Images were photographed with a 40x lens. Scale bars, 50 μm.

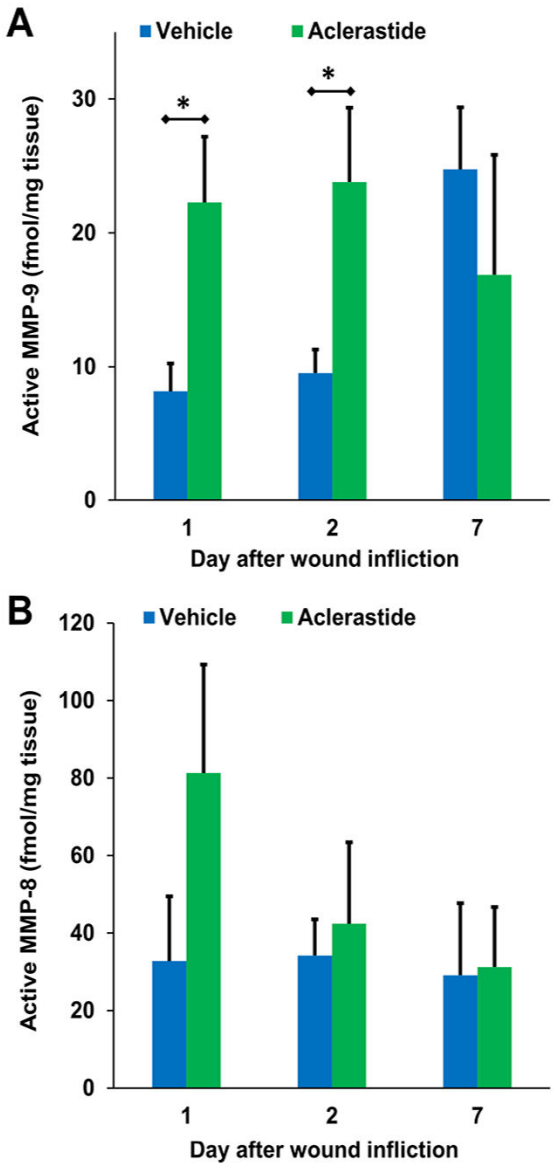

Fig. 4.

Aclerastide treatment results in upregulation of active MMP-9. Quantitative analysis of wound tissues using the affinity resin coupled with proteomics. Mean ± S.D., n = 3 mice per group per time point, $*P < 0.05$ by Student's *t* two-tailed test. A. Active MMP-9 is upregulated in aclerastide-treated wounds, resulting in 2.7- and 2.5-fold increases on days 1 and 2, respectively. B. No statistically significant differences were observed in the levels of active MMP-8 in aclerastide-treated wounds compared to vehicle-treated ones ($P = 0.08$).

Table 1.

Quantification of active MMPs in mouse wound samples[a]

Q1 Precursor *m/z*	Q3 Product *m/z*	MMP-8 Peptide
873.92 $[M+2H]^{2+}$	959.56 $[M+H]^{+}$ y9	
873.92 $[M+2H]^{2+}$	1218.64 $[M+H]^{+}$ yl2	[C]GVPDSGDFLLTPGSPK
873.92 $[M+2H]^{2+}$	**1430.72 $[M+H]^{+}$ yl4**	
534.76 $[M+2H]^{2+}$	639.32 $[M+H]^{+}$ y5	
534.76 $[M+2H]^{2+}$	753.37 $[M+H]^{+}$ y6	DISNYGFPR
534.76 $[M+2H]^{2+}$	**840.40 $[M+H]^{+}$ y7**	
500.26 $[M+2H]^{2+}$	618.35 $[M+H]^{+}$ y6	
500.26 $[M+2H]^{2+}$	**705.38 $[M+H]^{+}$ y7**	FFSLAETGK
500.26 $[M+2H]^{2+}$	852.45 $[M+H]^{+}$ y8	
		MMP-9 Peptide
832.94 $[M+2H]^{2+}$	1033.57 $[M+H]^{+}$ y9	
832.94 $[M+2H]^{2+}$	1090.59 $[M+H]^{+}$ y10	AFAVWGEVAPLTFTR
832.94 $[M+2H]^{2+}$	**1276.67 $[M+H]^{+}$ y11**	
622.34 $[M+2H]^{2+}$	704.41 $[M+H]^{+}$ y6	
622.34 $[M+2H]^{2+}$	**761.43 $[M+H]^{+}$ y7**	GSPLQGPFLTAR
622.34 $[M+2H]^{2+}$	889.49 $[M+H]^{+}$ y8	
549.00 $[M+3H]^{3+}$	642.4 $[M+H]^{+}$ y6	
549.00 $[M+3H]^{3+}$	979.6 $[M+H]^{+}$ y9	LGLGPEVTHVSGLLPR
549.00 $[M+3H]^{3+}$	**767.4 $[M+H]^{+}$ b8**	

[a]Quantification was done using three peptides per proteinase. In the first quadrupole (Q1), precursor *m/z* ions are selected and fragmented in second quadrupole (Q2), where a specific fragment is monitored in the third quadrupole (Q3). Denoted in bold in Q3 are the fragments used as 'quantifier' for each proteinase. The fragments in Q3 are assigned with conventional peptide fragmentation nomenclature. [C] = alkylated cysteine.